The significance of high-order dynamics in lap time simulations

Roberto Lot
Faculty of Engineering and the Environment, University of Southampton, United Kingdom

Nicola Dal Bianco
Department of Industrial Engineering, University of Padova, Italy

ABSTRACT: This work aims to study which level of detail should be preserved in the multibody modelling of a racing car in order to obtain reliable results without excessive model complexity. Three multibody models have been developed and compared through optimal control simulations. The models differ from each other for the order of dynamics comprised: starting from a 14 degrees of freedom (dof) car which includes chassis and wheels motion, a 10 dof model model is obtained by neglecting the wheels hop dynamics, finally a 7 dof model is derived by completely eliminating the suspension motion. Optimal control problem simulations, including parametric analyses varying the center of mass position and suspensions stiffness, have been executed on a full lap on the International circuit of Adria. Simulations results show that the 10 dof model gives almost the same results of the 14 dof one, while significantly reducing the computing time. On the contrary, the basic 7 dof model highlights remarkable differences in both the parametric analysis, suggesting the dynamics has been over-simplified.

Keywords: Lap time simulations, optimal control, car, dynamics, multibody, modelling, optimal maneuverer,

1 INTRODUCTION

Optimal control calculus for road vehicles have been widely used in recent years to calculate circuit lap times of vehicles and to find optimality of set up parameters. Computing power of modern computers, together with considerable improvements in solving algorithms, allows utilizing complex models that can reproduce quite accurately real vehicles dynamics. However, high fidelity models which are used for multibody simulations are usually too complicated for entire lap time simulations and simplified models are generally preferred. For example, [Perantoni 2014] uses a single mass car model with three degree of freedom (dof), that are yaw and translation along x and y-axis, tyre loads have been calculated by quasi steady state assumptions. A similar model has been adopted in [Kelly 2008], where the main chassis has the same dof but tyres rotational dynamic is also implemented. In this configuration, a full lap time simulation at Jerez circuit took approximately 8 hours on an Intel T7700 2.4GHz processor. In the same work, suspensions-related dof and a temperature-dependent tyre model have also been considered. Both in [Kelly 2008] and [Perantoni 2014], nonlinear programming algorithms are used. Different approaches have been adopted in [Tavernini 2013 and 2014] where the car is represented by a single-track still with three dof for the main chassis and two more dof for the tyre spin dynamics. In these two works an indirect method to solve optimal control problem has been adopted. A single-track model with fixed driving line can be found in [Thommyppillai 2009]: again chassis roll, pitch and vertical displacement motion are not considered. A linear quadratic preview algorithm has been used to compute the solution. Motorcycles performance also have been studied with optimal control simulations, and the first example can be found in [Cossalter 1999]. In such work a simple bike model composed of a single body is used to simulate the optimal manoeuvre on the Lucco-Poggio Secco curves (Mugello track). An enhanced bike model, that includes suspensions motion, is then described in [Cossalter 2013] and a full simulated lap on the circuit of Valencia

is compared with experimental data. The modelling of suspension motion is indeed quite relevant for motorbikes models because it significantly affects tyre loads both in transients and steady state conditions.

It is not clear what level of accuracy such simplified models may provide, nor what are the most important vehicle features that should be included for an accurate results. Multiple choices for the desired model structure can be made and different approximations can be assumed. As shown in previous examples taken from literature, common simplifications usually affect wheels, suspensions and/or chassis dynamics. Even controls that simulate drivers input can be inserted into the model at different levels of the dynamic. For instance, traction control can relies, in order of complexity, in tyre forces, wheels slip, or axle torque. Generally, the highest complexity is adopted in the particular dynamic that has to be investigated, while reasonable simplifications are taken in the rest of the model. However, a deep understanding of consequences of such approximations is still missing in literature, and how they affect simulation results is yet not well quantifiable.

The aim of this work is to study how different levels of detail in the modelling of car dynamics can influence both result outcomes and computational cost of dynamic lap time simulation, in order to understand which complexity should be adopted to get the best compromise between reliable results and short computational times. We developed a state-of-the-art model of a GT class sports car together with other two simpler models in order to study the differences between them. The full features model is composed by the car chassis which is a rigid bodies with 6 dof (translation and rotations in three space dimensions), then each wheel has two additional dof, respectively the suspension motion and wheel spin. In total the car has 14 dof. Then, a second model has been derived by suppressing the wheels vertical motion and a third one has been derived by further suppressing chassis yaw, pitch and vertical displacement. Mathematical models have been developed by using computer algebra software MBSymba^{TM}, which is a multibody library [Lot 2004] developed in Maple environment. Then, XOptima libraries have been used to generate C++ source file for the optimal control problem indirect formulation and Mechatronix libraries have been utilized to solve the problem. This indirect method for solving optimal control problems has been described by [Bertolazzi 2009], and its capabilities have been demonstrated both for four [Tavernini 2013 and 2014] and two [Cossalter2013] wheeled vehicles.

2 CARS MATHEMATICAL MODELLING

We developed a model of a GT class sports car together with other three simpler models, as described in the next sections. All models have been developed with Computer Algebra Systems and in particular by using MBSymba^{TM} [Lot 2004], which is available on the web `http://www.multibody.net/mbsymba`.

2.1 *Full features dynamic car model (14 dof)*

The full features model has 14 dof in total. As shown in figure 1, the gross motion is described by the centre of gravity speed V, the drift angle λ and the yaw rate Ω, the chassis motion include also the pitch μ and roll ϕ angles as well as the vertical motion z. Then, each wheel has two additional dof, respectively the suspension travel $z_{\theta\eta}$ (positive when the wheel lifts up) and the spin rate $\omega_{\theta\eta}$ (positive as the vehicle speed), with $\theta \in \{r, f\}$ indicating rear or front and $\eta \in \{r, l\}$ indicating right or left. Tyres loads are determined by tyres radial deformation, while tyre longitudinal and

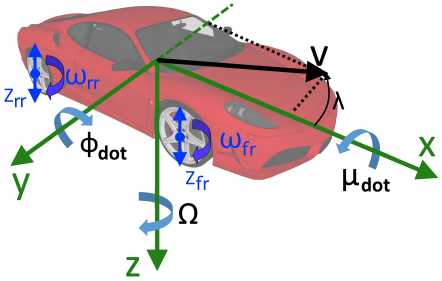

Figure 1.: 14 degrees of freedom car model.

lateral forces are calculated as function of the loads and slip quantities through a Pacejka magic formula. Drag and lift aerodynamic forces have been taken into account too. Controls relies in steering angle and wheel torques: positive torques are exerted only on the rear axle while negative ones (braking) are divided between front and rear wheels with a constant bias. A differential with torque distribution has been implemented in the rear axle. Since suspensions travel of GT cars is less than 40mm, travels $z_{\theta\eta}$ may be considered small, and consequently chassis variable ϕ, μ, z are small as well. Thus, all the expressions containing such variables and their derivatives have been approximated to the first order. By further assuming that drift and steering angles λ, δ are small too, the Newton equations for the chassis are the following:

$$m\left(\dot{V} + V\Omega\lambda\right) = S_{fl} + S_{fr} + S_{rl} + S_{rr} - (F_{fl} + F_{fr})\delta - F_D \tag{1a}$$

$$m\left(V\Omega - V\dot{\lambda} - \dot{V}\lambda\right) = S_{fl}\delta + S_{fr}\delta + F_{fl} + F_{fr} + F_{rl} + F_{rr} \tag{1b}$$

$$m\ddot{z} + m_{wf}\ddot{z}_{fl} + m_{wf}\ddot{z}_{fr} + m_{wr}\ddot{z}_{rl} + m_{wr}\ddot{z}_{rr} = mg - N_{fl} - N_{fr} - N_{rl} - N_{rr} - F_L \tag{1c}$$

where $S_{\theta\eta}, F_{\theta\eta}, N_{\theta\eta}$ are respectively the longitudinal, lateral and normal tyres forces on each wheel, F_D, F_L are respectively the drag and lift aerodynamics forces. The meaning and the value of all the constants that appear in these and the following equations are listed in table 1. Euler's rotation equations w.r.t the point **A** which lays below the centre of gravity at the road level are the following:

$$I_{xx}\ddot{\phi} + (-I_{xx}\mu + I_{zz}\mu - I_{xz})\dot{\Omega} - mh\dot{V}\lambda + I_{wf}\delta(\dot{\omega}_{fl} + \dot{\omega}_{fr}) = M_x(\phi, \mu, z, \dots) \tag{2a}$$

$$I_{yy}\ddot{\mu} + \phi(I_{yy} - I_{zz})\dot{\Omega} - m(h - z)\dot{V} - I_{wf}(\dot{\omega}_{fl} + \dot{\omega}_{fr}) - I_{wr}(\dot{\omega}_{rl} + \dot{\omega}_{rr}) = M_y(\phi, \mu, z, \dots) \tag{2b}$$

$$-I_{xz}\ddot{\phi} + (2\mu I_{xz} + I_{zz})\dot{\Omega} - \phi(I_{wf}(\dot{\omega}_{fl} + \dot{\omega}_{fr}) + I_{wr}(\dot{\omega}_{rl} + \dot{\omega}_{rr})) = M_z(\phi, \mu, z, \dots) \tag{2c}$$

where right hand side corresponds to the external force moments and for conciseness are not fully reported here, but the complete set of equations of motion are available at the link `http://www.multibody.net/mbsymba/vehicles/gtcar14dof`.

The equation governing the vertical dynamics of the rear right wheel is the following:

$$m_{wr}\dot{z}_{rr} - m_{wr}g + m_{wr}\ddot{z} + m_{wr}\ddot{\mu}b + m_{wr}\ddot{\phi}t_r = -N_{rr} - F_{s,rr} \tag{3a}$$

$$m_{wr}\dot{z}_{rl} - m_{wr}g + m_{wr}\ddot{z} + m_{wr}\ddot{\mu}b - m_{wr}\ddot{\phi}t_r = -N_{rl} - F_{s,rl} \tag{3b}$$

$$m_{wf}\dot{z}_{fr} - m_{wf}g + m_{wf}\ddot{z} - m_{wf}\ddot{\mu}a + m_{wf}\ddot{\phi}t_f = -N_{fr} - F_{s,fr} \tag{3c}$$

$$m_{wf}\dot{z}_{fl} - m_{wf}g + m_{wf}\ddot{z} - m_{wf}\ddot{\mu}a - m_{wf}\ddot{\phi}t_f = -N_{fl} - F_{s,fl} \tag{3d}$$

where t_r, t_f are respectively half of the rear and front track, $F_{s,\theta\eta}$ represent the suspension forces applied from the wheels to the chassis, i.e. a compressed suspension corresponds to a negative force. $F_{s,\theta\eta}$ is the sum of the spring, damper and anti-roll bar and is given by:

$$F_{s,\theta r} = k_{s\theta}z_{\theta r} + c_{s\theta}\dot{z}_{\theta r} + k_{j\theta}(z_{\theta r} - z_{\theta l}) \tag{4a}$$

$$F_{s,\theta l} = k_{s\theta}z_{\theta l} + c_{s\theta}\dot{z}_{\theta l} + k_{j\theta}(z_{\theta l} - z_{\theta r}) \tag{4b}$$

$$\tag{4c}$$

where $k_{s\theta}$, $c_{s\theta}$, $k_{j\theta}$ are respectively the (rear or front) spring, damper and anti-roll bar reduced stiffness. Moreover, the wheel spin dynamic equations are:

$$I_{wr}(\dot{\omega}_{rr} - \dot{\Omega}\phi - \Omega\dot{\phi}) = S_{rr}\left(\mu b + \phi t_r + z_{rr} + z - r_r\right) + T_{rr} \tag{5a}$$

$$I_{wr}(\dot{\omega}_{rl} - \dot{\Omega}\phi - \Omega\dot{\phi}) = S_{rl}\left(\mu b - \phi t_r + z_{rl} + z - r_r\right) + T_{rl} \tag{5b}$$

$$I_{wf}(\dot{\omega}_{fr} - \dot{\Omega}\phi - \Omega\dot{\phi}) = S_{fr}\left(-\mu a + \phi t_f + z_{fr} + z - r_f\right) + T_{fr} \tag{5c}$$

$$I_{wf}(\dot{\omega}_{fl} - \dot{\Omega}\phi - \Omega\dot{\phi}) = S_{fl}\left(-\mu a - \phi t_f + z_{fl} + z - r_f\right) + T_{fl} \tag{5d}$$

Table 1. Vehicle parameters

symbol	value	units	description
b	1.12	m	distance between the rear axle and the vehicle CoM
a	1.48	m	distance between the front axle and the vehicle CoM
$p = a + b$	2.6	m	wheelbase
h	0.4	m	CoM height
$2t_f$	1.71	m	front track
$2t_r$	1.62	m	rear track
M	1400	kg	total mass
I_x	400	kgm^2	x-axis vehicle inertia (w.r.t. CoM)
I_y	2000	kgm^2	y-axis vehicle inertia (w.r.t. CoM)
I_z	1320	kgm^2	z-axis vehicle inertia (w.r.t. CoM)
m_{wf}	15	kg	front wheel unsprung mass
m_{wr}	17	kg	rear wheel unsprung mass
I_{wf}	1.1	kgm^2	front wheel spin inertia
I_{wr}	1.3	kgm^2	rear wheel spin inertia
r_f, r_r	0.29	m	nominal wheel radius
k_{sf}	200e3	N/m	front spring stiffness
k_{sr}	180e3	N/m	rear spring stiffness
k_{jf}	140e3	N/m	front anti-roll bar stiffness
k_{jr}	120e3	N/m	rear anti-roll bar stiffness
k_{tf}, k_{tr}	200e3	N/m	tyres radial stiffness
c_{tf}, c_{tr}	150	Ns/m	tyres radial damping
c_D	0.34		aerodynamics drag coefficient
c_L	0		aerodynamics lift coefficient
β	0.7		braking bias
k_d	1e2	$Nmsrad^{-1}$	differential stiffness
N_0	5000	N	tyre nominal vertical load
μ_{xf}	1.57		front tyre max longitudinal adherence at nominal load
μ_{xr}	1.56		rear tyre max longitudinal adherence at nominal load
μ_{yf}	1.41		front tyre max lateral adherence at nominal load
μ_{yr}	1.51		rear tyre max lateral adherence at nominal load
K_{yf}	25	rad^{-1}	front tyre sidelsip stiffness at nominal load
K_{yr}	31	rad^{-1}	rear tyre sidelsip stiffness at nominal load
K_{xf}	34		front tyre longitudinal stiffness at nominal load
K_{xr}	32		rear tyre longitudinal stiffness at nominal load

where $I_{w\theta}$ are the wheel spin inertia and $T_{\theta\eta}$ the traction or braking torque. It can be noted that the expression multiplying the longitudinal tyre force is the loaded radius of the tyre.

Wheel torques $T_{\theta\eta}$ are not independent each other. Indeed, the longitudinal dynamics is controlled by only one independent parameter, i.e. the overall driving torque T which is the combination of the engine and brakes torque.

$$T_{fr} = \beta f^-(T/2)\,\mathrm{sign}(\omega_{fr}) \tag{6a}$$

$$T_{fl} = \beta f^-(T/2)\,\mathrm{sign}(\omega_{ff}) \tag{6b}$$

$$T_{rr} = (1-\beta) f^-(T/2)\,\mathrm{sign}(\omega_{fr}) + f^+(T/2) + k_d(\omega_{rl} - \omega_{rr}) \tag{6c}$$

$$T_{rl} = (1-\beta) f^-(T/2)\,\mathrm{sign}(\omega_{ff}) + f^+(T/2) - k_d(\omega_{rl} - \omega_{rr}) \tag{6d}$$

where sign is the (regularized) *signum* function, β is the front braking bias, f^- and f^+ return respectively the (regularized) negative and positive part of the argument, finally k_d is the differential stiffness. It can be observed that at the front wheel only negative torques (braking) can be applied, while at the rear ones both positive (traction) and negative are allowed, moreover the simultaneous presence of driving torque at the rear axle and braking torque at the front one is not allowed.

Tyres vertical load may be easily calculated as a function of tyres deformation, for simplicity it is assumed that elastic and damping forces are linear:

$$N_{\theta\eta} = \max\left(N_{\theta\eta 0} + k_{t,\theta\eta}\xi_{\theta\eta} + c_{t,\theta\eta}\dot{\xi}_{\theta\eta}, 0\right) \tag{7}$$

where $N_{\theta\eta 0}$ is the static tyre load, k_t the tyre stiffness, c_t the tyre damping coefficient and $\xi_{\theta\eta}$ the deformation variation from static configuration. For the rear right tyre we have:

$$\xi_{rr} = \mu b + \phi t_r + z_{rr} + z \tag{8}$$

and analogous expressions holds for the other tyres. Longitudinal and lateral tyre forces have been calculated as function of the tyre load N, the sideslip λ and longitudinal slip κ according to the Magic Formula Tyre Model [Pacejka 2002, ch. 4]. Tyre forces delay are modelled with first order relaxation equations, however the relaxation is applied to the slip instead than to the force, for the rear right wheel relaxation equations are:

$$\frac{\sigma_x}{V - \Omega t_r}\dot{\kappa}_{rr} + \kappa_{rr} = \frac{\dot{\omega_r} r(r_r - b\mu - t_r\phi - z - z_{rr})}{V - t_r\Omega + \dot{\mu}(h - r_r) + h\phi\Omega} - 1 \tag{9}$$

$$\frac{\sigma_y}{V - \Omega t_r}\dot{\lambda}_{rr} + \lambda_{rr} = \frac{b\Omega + h\dot{\phi} + V\lambda - (h - r_r)\Omega\mu}{V - t_r\Omega + \dot{\mu}(h - r_r) + h\phi\Omega} \tag{10}$$

In conclusion, chassis, wheels and tyre equations may be reduced to an implicit first order formulation as follows:

$$\boldsymbol{A}(\boldsymbol{x})\dot{\boldsymbol{x}} = \boldsymbol{f}(\boldsymbol{x}, \boldsymbol{u}, t) \tag{11}$$

where, for the 14 dof model, the state variable vector includes the following 29 variables:

$$\boldsymbol{x}_{14} = \{V, \lambda, \Omega, z, \phi, \mu, z_{dot}, \phi_{dot}, \mu_{dot}, \omega_{\theta\eta}, z_{\theta\eta}, z_{dot,\theta\eta}, \lambda_{\theta\eta}, \kappa_{\theta\eta}\}^\top \tag{12}$$

and the control input has 2 variables:

$$\boldsymbol{u} = \{T, \delta\}^T \tag{13}$$

2.1.1 *Natural frequencies*

The natural frequencies of the model so far described are reported in table 2, where they are calculated at a fixed speed of $V = 30\ m/s$ and in straight motion $\Omega = 0$. Natural frequencies of other two models that will be described in the next paragraphs are shown too. It can be noticed that the spin of the wheels is the fastest dynamics, while the wheels hop is slower, chassis motions and weave are the lowest. The higher the frequencies are, the more difficult is numerically to find the solution of the optimal control problem. A first option would be to neglect the wheel spin dynamics, i.e. to assume $I_{wr} = I_{wf} = 0$. However, in order to calculate longitudinal tyre forces it is still necessary to keep spin rates $\omega_{\theta\eta}$ as state variables. In other words, wheel spin equations (5) cannot be eliminated and have to remain as algebraic equations. But the indirect formulation that is used in this paper to solve the minimum lap time problem strictly requires an ODE problem formulation (section 3), so this possibility has not been exploited. Nevertheless, there are at least two other simplifications that may be sequentially introduced into the model: the first one is to neglect the vertical dynamics of the wheels, the second one is to neglect the chassis dynamics associated to the suspensions. These models are described more in detail in the next sections.

Table 2. Car natural frequencies

	full (14 dof)	massless-wheels (10 dof)	basic (7 dof)
weave	2.7 Hz	2.7 Hz	2.6 Hz
bounce	2.6 Hz	2.6 Hz	–
roll	5.1 Hz	4.9 Hz	–
pitch	3.2 Hz	3.1 Hz	–
wheels hop	20 ÷ 30 Hz	–	–
wheels spin	45 Hz	45 Hz	45 Hz

2.2 *Massless wheel model (10 dof)*

Wheels are responsible of the so-called *hop modes* which have a frequency range of $20 - 30$ Hz. If we neglect the wheel mass in the vertical dynamic equation (3), the force exerted by each suspension exactly balanced by the tyre vertical load. If we also neglect damping for a while, wheel hop equation (3) becomes algebraic and linear, so we can easily calculate the suspension travel as a function of the other state variables as follows:

$$z_{rr} = -\frac{k_{tr}(bk_{er}\mu + k_{er}z + 1/2\phi t_r k_{tsr})}{k_{tsr}k_{er}} \tag{14a}$$

$$z_{rl} = -\frac{k_{tr}(bk_{er}\mu + k_{er}z - 1/2\phi t_r k_{tsr})}{k_{tsr}k_{er}} \tag{14b}$$

$$z_{fr} = \frac{k_{tf}(ak_{ef}\mu - k_{ef}z - 1/2\phi t_f k_{tsf})}{k_{tsf}k_{ef}} \tag{14c}$$

$$z_{fl} = \frac{k_{tf}(ak_{ef}\mu - k_{ef}z + 1/2\phi t_f k_{tsf})}{k_{tsf}k_{ef}} \tag{14d}$$

where $k_{ts\theta} = k_{t\theta} + k_{s\theta}$ and $k_{e\theta} = k_{j\theta} + (k_{s\theta} + k_{t\theta})/2$. In particular it can be noticed that $z_{\theta\eta}$ are linear expressions of z, ϕ, μ. To preserve the damping characteristics of the pitch, bounce and roll chassis modes, the damping coefficients $c_{s\theta}$ of the suspensions has been replaced with $c_{e\theta}$, that is an approximated equivalent damping which preserve the damping ration of the chassis vibrations modes. After the elimination of wheel hop equations and suspension travel variables, the first order formulation (11) of the 10 dof model has 21 state variables:

$$\boldsymbol{x}_{10} = \{V, \lambda, \Omega, z, \phi, \mu, z_{dot}, \phi_{dot}, \mu_{dot}, \omega_{\theta\eta}, \lambda_{\theta\eta}, \kappa_{\theta\eta}\}^T \tag{15}$$

2.3 *Basic car model (7 dof)*

This model neglects the chassis motion due to the suspensions, i.e. variables z, ϕ, μ are set to zero and equations (1c), (2a), (2c) are discarded. Therefore there remain only 7 dof: gross motion variables V, λ, Ω and wheels spin variables $\omega_{\theta\eta}$. However, the introduction of such simplifications determines the loss of information (i.e. the equations) necessary to calculate tyre loads $N_{\theta\eta}$. To solve this problem, tyre loads in steady state conditions are pre-calculated as a function of the longitudinal speed V, longitudinal acceleration a_x and lateral acceleration a_y:

$$N_{\theta\eta} = N_{\theta\eta}(V, a_x, a_y) \tag{16}$$

More precisely, the full features dynamic model is converted into a steady state problem by considering only the right hand side of equations (11), moreover a fictitious longitudinal gravity field has been introduced to emulate longitudinal acceleration a_x, while the steady state lateral acceleration is simply $a_y = \Omega V$. The quasi static problem has 29 algebraic equations and 32 variables: states 12, inputs 13 and acceleration a_x. In conclusion, once variables V, a_x, Ω have been fixed, all other variables may be calculated from steady state equations (provided that a solution exists).

To finally utilize quasi-static expression (16) in the 7 dof dynamic model it is necessary to calculate the longitudinal and lateral accelerations as a function of state variables, the easiest solution is to introduce a_x and a_y as a new state variable and the following first order low pass filter on the actual vehicle acceleration:

$$\tau_{ax}\dot{a}_x + a_x = \dot{V} + \Omega V\lambda \tag{17}$$

$$\tau_{ay}\dot{a}_y + a_y = \Omega V - \dot{V}\lambda - V\dot{\lambda} \tag{18}$$

where τ_{ax} and τ_{ay} are the filter time constants. Such filters introduce an artificial time lag between tyre loads and vehicle acceleration variations, however this could be considered as a simplified description of the time lag which is naturally induced by suspensions in real vehicles.

In conclusion, the first order formulation (11) of the 7 dof model has 17 state variables:

$$\boldsymbol{x}_7 = \{V, \lambda, \Omega, a_x, a_y, \omega_{\theta\eta}, \lambda_{\theta\eta}, \kappa_{\theta\eta}\}^T \tag{19}$$

3 FORMULATION OF THE MINIMUM LAP TIME PROBLEM

The minimum lap time problem consists in finding the vehicle control inputs that minimize the time T necessary to move the vehicle along the track from the starting line to the finish one. From a mathematical point, the problem may be formulated as follows:

$$\text{find:} \quad \min_{\boldsymbol{u} \in \boldsymbol{U}} T \tag{20a}$$

$$\text{subject to:} \quad \boldsymbol{A}\dot{\boldsymbol{y}} = \boldsymbol{f}\left(\boldsymbol{y}, \boldsymbol{u}, t\right) \tag{20b}$$

$$\boldsymbol{\psi}\left(\boldsymbol{y}, \boldsymbol{u}, t\right) \leq \boldsymbol{0} \tag{20c}$$

$$\boldsymbol{b}\left(\boldsymbol{y}(0), \boldsymbol{y}(T)\right) = \boldsymbol{0} \tag{20d}$$

where $\boldsymbol{x}$ and $\boldsymbol{u}$ are respectively the state variables and inputs vector, (20b) is the state space model, (20d) is the set of boundary conditions used to specify the vehicle state at the beginning and at the end of the manoeuvre and (20c) are algebraic inequalities that may bound both the state variables and control inputs. Since we do not use a predefined vehicle trajectory, but we calculate the racing line the optimization, the state space model (20b) actually include the car model (11) to the track one. The latter is based on a curvilinear coordinates approach and it is described in detail in [Lot 2014]. A constraint is used to prevent that the vehicle exits from the track:

$$-(w_t - t_w) < n < w_r - t_w \tag{21}$$

where n is the car lateral position w.r.t. the track reference line, t_w is the half width of the car and w_r, w_l are respectively the right and left width of the track. Another constrain is used to limit the traction torque T to maximum engine torque available T_a as follows:

$$T < T_a\left(\tfrac{\omega_{rr}+\omega_{rl}}{2}\right) \tag{22}$$

It should be noted that T_a is the torque available at the rear axle, assuming that the proper gearbox ratio is used while driving.

The OCP formulation (20) is general and the problem may be solved by using different approaches [Bryson 1999], in this case the indirect approach which convert the OCP into a two-points boundary value problem is used, as described in [Bertolazzi 2005 and 2006], [Tavernini 2014], [Lot 2015].

4 SIMULATION RESULTS AND DISCUSSION

The three models described in section 2 have been compared on a full lap simulation on the International circuit of Adria (`www.adriaraceway.com`). The trajectory resulting from 14 dof model simulation is illustrated in figure 2a, while the vehicle speed and accelerations are shown in figure 2b. The maximum braking and lateral accelerations are of $\approx 15m/s^2$, while the maximum positive longitudinal one is $\approx 10m/s^2$, limited by the engine power limit. The simulated lap time is of $73.789s$, which is not so different from a qualifying lap-time of the GT1 series. The computational time for a single simulation is respectively $\approx 1700s$ on a standard PC equipped with an Intel *Core 2 Quad* Q9300 CPU. Simulations have been repeated for the 10 dof and 7 dof models, finding simulated lap times respectively of $73.790s$ and $72.967s$, while the computational time was respectively $970s$ and $560s$. In other words, simplified models lead to a lap time prediction very similar to the one of the 14 dof model, but by using respectively the 57% and 33% of computational time. However, in lap time simulations it is more important to capture the lap time sensitivity to vehicle set-up variations that its absolute value, which is quite difficult to find because of the uncertainty of some parameters, first of all tyre adherence in real conditions. Thus we choose to test the accuracy of the three models through a comparison in two parametric analyses, rather than looking at the absolute lap-time for each model. The first parameter that has been changed is the longitudinal position of the centre of mass **G**: $1.12m < b < 1.26m$. The lap-times obtained with the three models are shown in figure 3a. The 14 dof model shows a kind of parabolic trend, with the best performance obtained for $b = 1.215m$. The 10 dof model lap-times are very close to that of the full one: the highest time difference is of $\approx 0.01s$ and the minimum time also is reached at the same value of b. Differently, the basic 7 dof model shows some discrepancies with respect to the other two models: the lap-times are at significantly lower

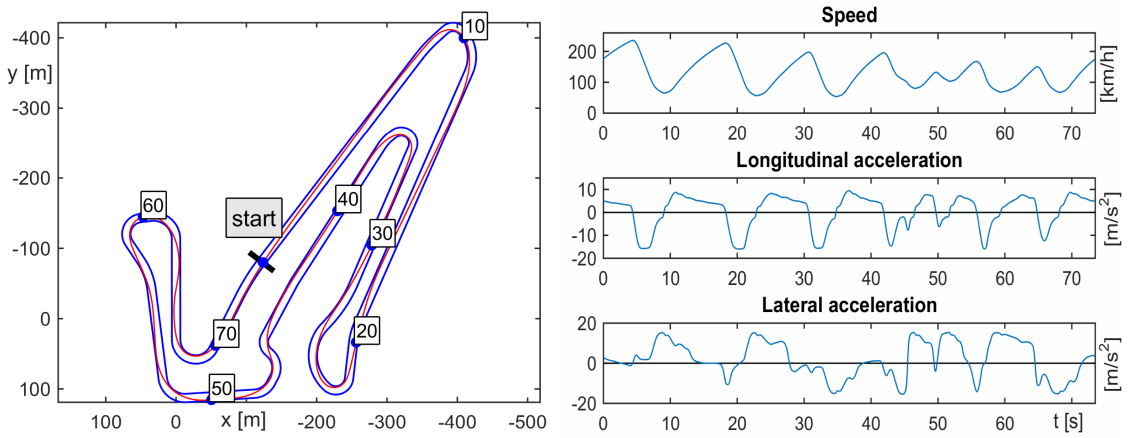

(a) Trajectory

(b) Gross-motion

Figure 2.: Trajectory and gross-motion resulting from optimal control simulation on the circuit of Adria. The track is treaded clockwise.

and, more important, the minimum time is obtained at a different position of **G**, precisely for $b = 1.155m$.

In the second parametric analysis, the stiffness of the front suspensions spring has been varied in the range $160e3N/m < k_{sf} < 240e3N/m$, and the calculated lap-times are shown in figure 3b. Again, the lap-times obtained with the full and massless-wheel models are very close, and the minimum time is obtained for the lowest value of the spring stiffness (while the absolute minimum seems to be located outside interval of analysis). In the range of stiffness considered, the lap-times varies of $\approx 0.1s$ between the lowest and the highest. On the contrary, the basic model appears to be less sensitive to changes of the suspension stiffness, with lap-times varying of only $0.01s$ in the same range of stiffness. Moreover, a minimum time is shown for $k_{sf} = 180e3N/m$. Since the main difference between the three models lays in the way tyres load are calculated, the results of the previous analyses suggest that the steady state map approach adopted for the basic model does not manage to faithfully reproduce the tyres loads on the wheels. In order to demonstrate this, we performed a simulation with the basic model at fixed trajectory; the trajectory imposed is the one obtained with the full model. The load on the rear right tyre resulting from this simulation is shown in figure 4. The massless-wheel model is also reported, even if the trajectory has not been imposed for this model. Figure 4 highlight a difference of up to $1e3N$ between the basic and full model, while the massless-wheel one differs up to only $80N$ (still from the full one).

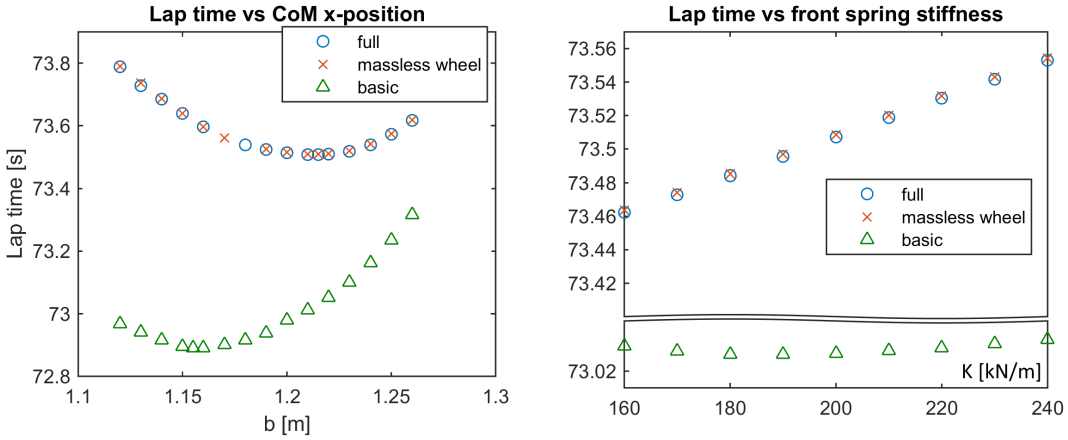

(a) Parametric analysis of the x-position of the CoM b (the reference value is $b = 1.120m$).

(b) Parametric analysis of the stiffness of the front suspensions spring k_{sf} (reference is $k_{sf} = 200e3N/m$).

Figure 3.: Parametric analyses comparison of the three models.

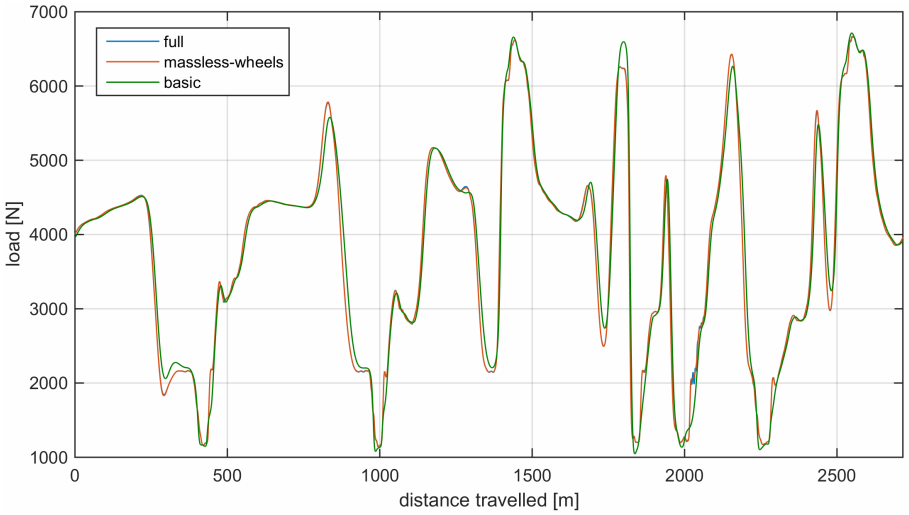

Figure 4.: Load on the rear right wheel. The full model line is not visible because it is overlapped by the massless-wheels model line. In the basic model simulation the trajectory of the full model has been imposed in order to remove trajectory-related load differences.

This latter result, together with the parametric analyses, suggests that the the massless-wheel 10 dof model represents a reasonable simplification of the full one, since it reduces the computing time of simulations and at the same time it keeps a good accuracy of the general dynamics (in particular of tyres load). Differently, the basic 7 dof model shows a different behaviour in both the parametric analysis, thus we can conclude that the model is over-simplified. It might be possible that the differences between the three levels of modelling can increase or diminish if the specifications of a different car category are used. However, we have showed that there are differences between the models and we also have a given a rough quantification of them.

5 CONCLUSIONS

In this work a 14 dof multibody car model has been developed: such model considers the chassis as a rigid body with 6 dof and includes wheels vertical motion and spin rotation too. Moreover two other models, with simplified dynamics, have been derived form the first one: a 10 dof model where the wheel mass is neglected and a basic 7 dof model where the chassis motion due to suspensions is neglected too. The aim of these latter models is to provide simpler tools to be used in optimal control simulation without losing in accuracy of the car dynamics.

These models have been then compared through optimal control simulations on the circuit of Adria. Results exposed in section 4 showed that the massless model gives almost the same outcomes of the full one both in the simulated lap-time and in the two parametric analyses performed. In addition, a reduction of the 43% in the computing time has been measured. Differently, the basic model highlighted remarkable differences since in the two parametric analysis the best performance is achieved for different position of the CoM and different front spring stiffness than the other models. Moreover, even imposing on the basic model the exact trajectory obtained through the full one, significant differences in the tyre loads have been demonstrated. Thus, despite the computing time for the basic model is the lowest (67% less than the full one) we can claim that the best compromise between simulation speed and accuracy of the results is represented by the massless model.

Finally, we recall that the two simplified models still include the fastest dynamics, that is the one related wheel spin. This because of the non feasibility of using algebraic equations in the indirect formulation for the optimal control problem. A further perspective could be the developing of a model that exclude such dynamics without loosing in accuracy.

REFERENCES

Bertolazzi E., Biral F. & Lio D.M. 2005: Symbolic - numeric indirect method for solving optimal control problems for large multibody, *Multibody System Dynamics*: 13 233252.

Bertolazzi E., Biral F., Lio D.M. & Cossalter V. 2007: Influence of riders upper body motions on motorcycle Minimum time maneuvering, *Conference paper at ECCOMAS Thematic Conference*.

Bryson A.E. 1999: Dynamic optimization, *Addison Wesley Longman*.

Cossalter V., Lio D.M., Lot R. & Fabbri L. 1999: A general method for the evaluation of vehicle manoeuvrability with special emphasis on motorcycles, *Vehicle System Dynamics*: 31,2, 113-135.

Cossalter V., Lot R. & Tavernini D. 2013: Optimization of the centre of mass position of a racing motorcycle in dry and wet track by means of the Optimal Maneuver Method, *IEEE International Conference on Mechatronics, ICM 2013, Vicenza (ITALY)*.

Kelly D.P. 2008: Lap time simulation with transient vehicle and tyre dynamics, *PhD thesis*: Bedford, Cranfield, University, School of Engineering.

Lot R. & Biral F. 2014: A curvilinear abscissa approach for the lap time optimization of racing vehicles, *19th IFAC World Congress on International Federation of Automatic Control, Cape Town*.

Lot R. & Bianco N.D. 2015: Lap Time Optimization of a racing go-kart, *Vehicle System Dynamics*: to appear.

Lot R. & Lio D.M. 2004: A symbolic approach for automatic generation of the equations of motion of multibody systems, *Multibody System Dynamics*: 12,2, 147-172.

Pacejka H.B. 2002: Tyre and vehicle dynamics, *Butterworth Heinemann*: ISBN 0 7506 5141 5.

Perantoni G. & Limebeer D.J.N. 2014: Optimal control for a Formula One car with variable parameters, *Vehicle System Dynamics*: 52,5, 653-678.

Tavernini D., Massaro M., Velenis E., Katzourakis D.I. & Lot R. 2013: Minimum time cornering: the effect of road surface and car transmission layout, *Vehicle System Dynamics*: 51:10, 1533-1547.

Tavernini D., Velenis E., Lot R. & Massaro M. 2014: The optimality of the handbrake cornering technique, *ASME*: 136.

Thommyppillai M., Evangelou S.A. & Sharp R.S. 2009: Car driving at the limit by adaptive linear optimal preview control, *Vehicle System Dynamics*: 479 15351550.